ANNALS OF MEDICINE
2025, VOL. 57, NO. 1, 2470958
https://doi.org/10.1080/07853890.2025.2470958

RESEARCH ARTICLE

OPEN ACCESS Check for updates

Sodium butyrate alleviates DSS-induced inflammatory bowel disease by inhibiting ferroptosis and modulating ERK/STAT3 signaling and intestinal flora

Yingyin Liu*, Nachuan Chen*, Huaxing He, Lulin Liu and Suxia Sun

Department of Nutrition and Food Hygiene, Guangdong Provincial Key Laboratory of Tropical Disease Research, School of Public Health, Southern Medical University, Guangzhou, Guangdong, China

ABSTRACT

Background: Inflammatory bowel disease (IBD), encompassing Crohn's disease (CD) and ulcerative colitis (UC), can seriously impact patients' quality of life. Sodium butyrate (NaB), a product of dietary fiber fermentation, has been shown to alleviate IBD symptoms. Some studies have shown that it is related to ferroptosis. However, the precise mechanism linking NaB, IBD, and ferroptosis is not clear.

Objective: This study aimed to demonstrate that NaB suppresses ferroptosis, thereby alleviating inflammatory bowel disease (IBD) through modulation of the extracellular regulated protein kinases/signal transducer and activator of transcription 3 (ERK/STAT3) signaling pathway and intestinal flora.

Methods: An IBD model was established using 2.5% (*w/v*) dextran sulfate sodium (DSS). Mice were orally administered low-dose NaB, high-dose NaB , or 5-aminosalicylic acid (5-ASA). Ferroptosis-related molecules were measured using specific kits, and western blotting (WB) and real-time polymerase chain reaction (RT-qPCR) were used to determine the levels of the target molecules.

Results: NaB alleviated symptoms in IBD mice, including reduced weight loss, prolonged colon length, reduced disease activity index (DAI), and reduced spleen index and mRNA expression of inflammatory factors. Additionally, NaB reduced the content of Fe^{2+} and myeloperoxidase (MPO) and increased the content of GSH and the activity of superoxide dismutase (SOD), which reflected NaB-inhibited ferroptosis. Moreover, western blotting showed that NaB enhanced STAT3 and ERK phosphorylation. In addition, NaB regulates the composition and functions of flora related to IBD.

Conclusion: NaB alleviates IBD by inhibiting ferroptosis and modulating ERK/STAT3 signaling and the intestinal flora.

ARTICLE HISTORY
Received 11 October 2024
Revised 14 January 2025
Accepted 6 February 2025

KEYWORDS: Sodium butyrate; IBD; ferroptosis; STAT3; ERK; gut microbiota

Introduction

Inflammatory Bowel Disease (IBD) encompasses ulcerative colitis (UC) and Crohn disease (CD). It is characterized by chronic inflammation of the intestinal mucosa, leading to debilitating symptoms and serious consequences [1]. The incidence of IBD is rising rapidly in Asia and study suggested that environmental or lifestyle factors related to industrialization may play a role [2]. Therefore, it is very important to explore the pathogenesis and prevention and treatment of inflammatory bowel disease. Some studies have pointed out that STAT3, the gene encoding which lies within an IBD-implicated locus, is activated in epithelial cells from patients with IBD, and IEC-specific Stat3 deletion affects epithelial repair [3]. However, the exact mechanism underlying IBD remains unclear and needs to be explored.

Sodium butyrate (NaB), a kind of short-chain fatty acids (SCFAs), is derived from dietary fiber produced by the breakdown of intestinal flora [4]. Studies have shown that butyrate plays a crucial role in regulating

CONTACT Suxia Sun suxiasun@hotmail.com Department of Nutrition and Food Hygiene, Guangdong Provincial Key Laboratory of Tropical Disease Research, School of Public Health, Southern Medical University, Guangzhou, Guangdong, China
Supplemental data for this article can be accessed online at https://doi.org/10.1080/07853890.2025.2470958.
*These authors have contributed equally to this work.

cell proliferation, apoptosis, and differentiation, which helps maintain the integrity of the colonic mucosa in mice, contributing to resistance against colitis [5]. In addition, many in-depth studies have been conducted on this mechanism. One study found that oral butyrate notably reduced leukocyte (eosinophil and neutrophil) infiltration in the colon mucosa and improved trophism [6]. Moreover, a previous study reported that butyrate significantly alleviated IBD and altered the expression of Slc16a1, Slc16a4, Slc5a8 and Abcg2 [7]. Despite this, the mechanism of action of NaB in IBD is not yet fully understood. Therefore, it still needs to be explored to optimize treatment.

Ferroptosis is a unique, iron-dependent form of non-apoptotic cell death, characterized by uncontrolled and overwhelming peroxidation of polyunsaturated fatty acids in membrane phospholipids, ultimately leading to rupture of the plasma membrane [8,9]. Ferroptosis is strongly correlated with various diseases including UC, although its exact pathophysiological role remains unclear [10]. Therefore, several studies have explored the correlation between IBD and ferroptosis. A previous study indicated that seliciclib alleviates UC by inhibiting ferroptosis and improving intestinal inflammation [11]. In addition, isorhamnetin induced ferroptosis-mediated colitis by activating the NRF2/HO-1 pathway and iron chelate [12]. Studies have shown that butyrate protects cells against oxidative stress and may inhibit ferroptosis, which reduces the ferroptosis marker H_2O_2 [13]. Therefore, ferroptosis is a promising therapeutic target for UC treatment.

Signal transducer and activator of transcription 3 (STAT3) has been identified as a key hub gene associated with ferroptosis in UC, based on research that identified STAT3 from a set of 13 hub genes derived from differentially expressed genes (DEGs) and ferroptosis-related genes [14]. Thus, there is a need to further explore the connection between the STAT3-regulated pathways, ferroptosis, and UC. UC is primarily associated with a dysregulated interplay between intestinal epithelial cells, microbial metabolites, and macrophages. Research suggests that restraint of extracellular regulated protein kinases1/2 (ERK1/2) reduces the beneficial effects of butyrate-primed macrophages, specifically diminishing their positive impact on goblet cell function [15]. STAT3 is phosphorylated by ERK at S727. Studies have shown that mitochondrial STAT3 phosphorylation at S727 by ERK inhibits mitochondrial ROS generation during reperfusion [16]. These findings suggest that the ERK/STAT3 signaling pathway may serve as a link between sodium butyrate, ferroptosis, and UC, but it has not been verified, which will be the focus of this study.

Moreover, modulation of gut flora by sodium butyrate is crucial for alleviating inflammatory bowel disease (IBD). For example, substances such as *Lycium barbarum* and riboflavin have been shown to modulate gut microbiota and alleviate UC by increasing the abundance of butyric acid in the gut [17,18]. In summary, this study aimed to investigate the roles of ferroptosis, ERK/STAT3 pathway, and gut microbiome in the amelioration of IBD by sodium butyrate.

To sum up, in this study, we will carry out a series of experiments to study the effects of sodium butyrate on ERK/STAT3, ferroptosis and the regulation of intestinal flora in the process of alleviating IBD, so as to provide a basis for the practical application of NaB and provide suggestions for the dietary therapy of IBD.

Materials and methods

Chemicals and reagents

A 2.5% dextran sulfate sodium (DSS) solution was prepared from DSS powder (25 g) and sterilized water (1000 mL). This solution was used immediately after preparation. For the low-dose and high-dose NaB groups, solutions were formulated by dissolving 0.05 g and 1 g of NaB powder per mL of sterilized water. The 5-aminosalicylic acid (5-ASA) group was prepared by dissolving 0.015 g 5-ASA powder in sterilized water. All mice were administered a standard intragastric administration of 0.1 ml/10 g body weight.

Animal experiments

Seven-week-old C57BL/6J male mice were obtained from Guangdong Experimental Animal Center. Randomization was employed to allocate 40 mice into 5 groups. Forty mice were divided into five groups: control ($n=8$), model ($n=8$), Low-dose NaB (NaB-L, $n=8$), High-dose NaB (NaB-H, $n=8$), and 5-ASA ($n=8$). The sample size was determined by a power analysis based on expected effect sizes and variability observed in preliminary studies. Following one week of acclimatization, Mice were included if they were aged 7 weeks and weighed between 19 and 21 g. Mice were excluded if they showed any signs of illness or injury before the experiment began.

From the first day to the third day, all the mice drink sterilized water. From the first day to the seventh day, to add a protective effect to the mice in both NaB groups, control group, model group and 5-ASA group were administrated saline, while mice of NaB-L group were administrated 500 mg/kg body weight NaB, mice of NaB-H group were administrated 1 g/kg body weight

NaB. Each mouse was administered at 0.1 ml/10g body weight. From the first day tothe third day, mice in the NaB groups were given NaB solution by intragastric administration. From the forth day to the ninth day, in order to create mouse model of IBD, sterilized water of Model group, NaB-L group, NaB-H group and 5-ASA group were replaced into 2.5% DSS water, mice of 5-ASA group were administrated 150 mg/kg body weight 5-ASA and the administration method for other groups remained the same as before. On the seventh day, all the 2.5% DSS water was replaced with sterilized water, and administration way of all the group were the same (Figure 1A). The entire animal experiment was conducted in the SPF animal Laboratory. All the administration was conducted in the afternoon and the weighing and DAI testing was done in the morning.

After a 12-hour fasting, all mice were euthanized and samples were collected, including blood, liver, spleen, colon, and colon contents. Photographs of the colons were taken, and organ weights and colon lengths were recorded. The spleens and colons were divided into two parts for −80 °C freezing and fixing. More detailed information about animal experiments is in the Supplementary Appendix.

Body weight and disease activity index (DAI) assessment

During the DSS modeling process, the body weights of the mice were measured daily at the same time to ensure consistency. In addition to body weight measurements, several other parameters were monitored, including changes in stool consistency and rectal bleeding. To assess the overall disease severity, the Disease Activity Index (DAI) was calculated using the following formula: DAI = (Weight loss score + Stool score + Bleeding score)/3. And the scoring criteria are shown in Table 1. This calculation provides a composite score that reflects the severity of the disease based on recorded changes in body weight, stool consistency, and rectal bleeding.

Histopathological examination

Hematoxylin and eosin (H&E) staining: For tissue analysis, spleen and colon tissues were carefully prepared by selecting sections 0.5 cm from the anus. Tissues were fixed to preserve their structural integrity. Following fixation, tissues were embedded in paraffin and sectioned into thin slices for detailed examination. H&E staining was performed on the tissue sections to highlight the different cellular components and reveal histopathological changes. The stained sections were then observed under a microscope to assess any pathological alterations and gain insight into the tissue conditions. And the pathological status of the colons were then score. The scoring criteria are shown in Table 2.

Alcian Blue-Periodic Acid Schiff (AB-PAS) staining

Alcian Blue-Periodic Acid Schiff (AB-PAS) staining was performed to assess mucosal integrity and goblet cell abundance in colon tissue sections. Tissues were fixed in 10% neutral-buffered formalin, embedded in paraffin, and sectioned into 5 µm slices. The sections were dewaxed in xylene, rehydrated through a graded series of ethanol to distilled water, and stained with 1% Alcian Blue solution (pH 2.5) for 30 min to identify acidic mucins. After rinsing, sections were treated with 0.5% periodic acid for 10 min to oxidize mucopolysaccharides, followed by incubation with Schiff reagent for 15 min to stain neutral mucins. The slides were counterstained with hematoxylin for 1–2 min, dehydrated through graded ethanol, cleared in xylene, and mounted with neutral resin. Eight random fields of stained sections of each group were observed under a microscope for goblet cell analysis and mucosal assessment. The number of goblet cells per crypt was calculated.

Immunohistochemistry analysis

Colon tissue sections were blocked with BSA at room temperature for 20 mins and then incubated with primary antibodies diluted 1000 times against ERK, p-ERK, STAT3 and p-STAT3 overnight at 4 °C. Next, the sections were incubated with diluted secondary antibodies at room temperature for 1 h. DAB staining was performed and the sections were counterstained with hematoxylin. Finally, the sections were mounted using a neutral resin. The average density of stained sections was measured.

Ferroptosis related indexes assessment

The activity of superoxide dismutase (SOD) and levels of Fe^{2+}, glutathione (GSH), and myeloperoxidase (MPO) were measured using specific assay kits to assess oxidative stress and inflammatory responses. Additionally, molecular analysis, including real-time polymerase chain reaction (RT-qPCR) and western blotting (WB), was performed to determine the mRNA expression and protein levels of key regulators involved in ferroptosis, including acyl-CoA synthetase

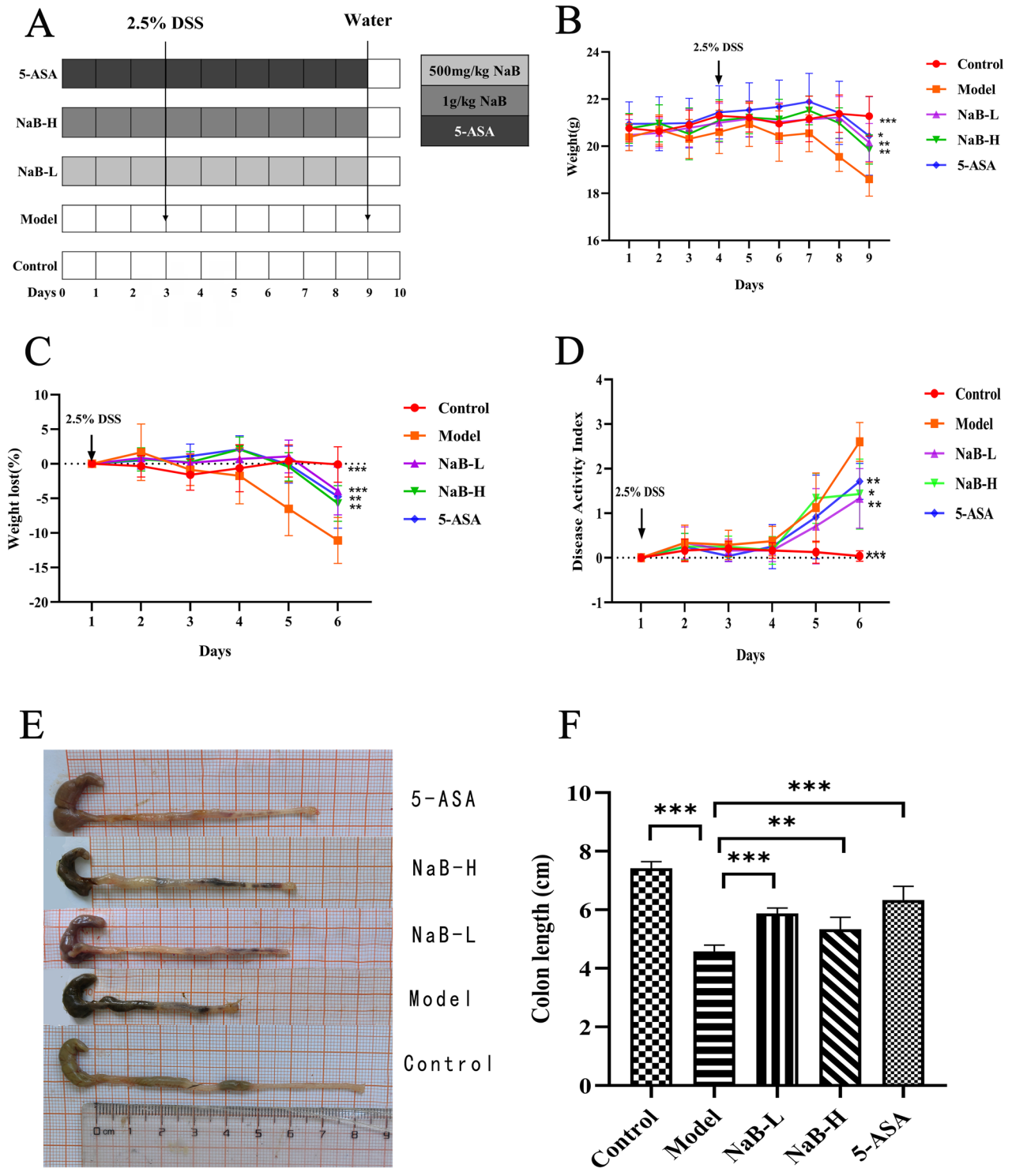

Figure 1. General condition of mice. (A) Experimental protocol for inflammation bowel disease model. (B) Body weight change of mice during the whole experimental period. (C) Body weight lost (%) during modeling period. (D) DAI change. (E) Photographs of representative colons of each group. (F) Average length of colons of each group. *$p < 0.05$; **$p < 0.01$; ***$p < 0.001$ vs. model.

long-chain family member 4 (ACSL4), Solute Carrier Family 7 member 11 (SLC7A11), and Glutathione Peroxidase 4 (GPX4), providing insights into the underlying mechanisms at both the transcriptional and translational levels.

Reverse transcription and real-time quantitative polymerase chain reaction (RT-qPCR)

To analyze mRNA expression in mouse colon tissue, total RNA was first extracted by placing the tissue in a centrifuge tube and processing it with Trizol,

Table 1. Scoring standards of the DAI value.

Items	Scoring standard	Scores
Weight loss (%)	No loss	0
	1–5	1
	6–10	2
	11–15	3
	>15	4
Stool	Normal	0
	Loose stool	2
	Diarrhea	4
Bleeding	No blood	0
	Occult blood positive	2
	Gross blood	4

Table 2. Histological scoring criteria.

Items	Scoring standard	Scores
Inflammation	None	0
	Mild	1
	Severe	2
Depth of lesion	None	0
	Submucosa	1
	Muscular layer	2
	Serosa	3
Recess destruction	None	0
	1/3 Of the basal recess destroyed	1
	2/3 Of the basal recess destroyed	2
	Only intact surface epithelium	3
	All crypts and epithelium destroyed	4
Extent of disease(%)	1–25	0
	26–50	1
	51–75	2
	76–100	3

chloroform, isopropanol, and ethanol. After extraction, RNA concentration and purity were measured to ensure quality, and the RNA was reverse-transcribed into cDNA following the TAKARA procedure. RT-qPCR was performed for quantitative analysis of mRNA. The qPCR conditions included an initial denaturation at 95 °C for 30 sec, followed by 40 cycles of denaturation at 95 °C for 15 sec, and annealing/extension at 60 °C for 30 sec, during which the fluorescence signal was collected. Finally, the relative expression levels of the target mRNA were calculated using the 2^−ΔΔCt method, allowing for a precise comparison of gene expression between samples. The primer sequences of each molecule are listed in Supplementary Table 1.

Western blot detecting protein expression level

Twenty milligrams of colon tissue was weighed and 300 µl of RIPA lysate containing 1% phosphatase inhibitor, 1% protease inhibitor, and 1%PMSF was added. After grinding with a low-temperature grinder, the tissue lysate was placed on ice for 30 mins and centrifuged. The total protein concentration was determined using the BCA protein quantification method, and the amount of Phosphate Buffer Saline (PBS) required for adding diluted protein and the amount of buffer were calculated accordingly. Finally, the samples were heated in a metal bath at 100 °C for 7 min.

The protein samples were separated on 10 and 12% sodium dodecyl sulfate-polyacrylamide gels. They were then transferred to PVDF membranes, blocked, and incubated with primary and secondary antibodies. A Tanon imaging system was used to develop and take pictures. ImageJ software was used to calculate the gray values of the protein strips. GAPDH was used as the internal reference protein, and the experiment was repeated three times.

16S rRNA amplicon sequencing

Conserved regions were targeted to design universal primers for PCR amplification of one or more highly variable regions of 16S rRNA. The amplified products were sequenced using the MiSeq/HiSeq platform with paired-end sequencing. Operational Taxonomic Unit (OTU) clustering was then performed on the highly variable region sequences. This was followed by species annotation and abundance, α-diversity, and β-diversity analysis. The specific process is as Supplementary Figure 1.

Statistical analysis

The results are expressed as the mean ± SD. Comparisons between two groups of averages were performed using two-tailed *t*-test or Mann–Whitney test, while comparisons between multiple groups of averages were performed using one-way ANOVA. SPSS software (version 25.0) was used for the statistical analysis of the data, and GraphPad Prism 8.0.1 was used for graph drawing. Statistical significance was set at $p < 0.05$. The assumptions of the statistical tests were checked and met. And all the results are showed in Supplementary Table 2.

Results

General condition of mice

To some extent, weight change, DAI, and colon length reflect the severity of IBD in mice. After the intervention of mice (Figure 1A), the general condition of mice is as follows. In the DSS-treated groups, mice began to show significant weight loss starting on the seventh day, and by the final day, the mice in the control, NaB-L, NaB-H, and 5-ASA groups were significantly heavier than those in the model group (Figure 1B) ($p < 0.001$; $p < 0.001$; $p < 0.01$; $p < 0.05$; $n = 8$) and had less weight loss (Figure 1C) ($p < 0.001$; $p < 0.001$; $p < 0.01$; $p < 0.05$; $n = 8$). On the fourth day of the modeling period, the DAI of mice that drank DSS increased

rapidly. On the last day, the DAI of the control, NaB-L, NaB-H, and 5-ASA groups was notably lower than that of the model group (Figure 1D) ($p < 0.01$; $p < 0.05$; $n = 8$). The colon length of the model group was significantly shorter than that of the control group, whereas the colon length in the two NaB intervention groups was significantly longer than that in the model group (Figure 1E,F) ($p < 0.001$; $p < 0.01$; $n = 5$). These results indicate that the IBD model has formed and that NaB can alleviate IBD.

NaB enhances immunity of mice and reduces inflammatory cytokine secretion

The spleen index reflects the immune system status of mice, and the expression level of inflammatory cytokine secretion reflects the inflammatory state of mice [19]. By looking at the HE-stained sections of the spleen, it can be observed that compared to the control group, the boundaries of red and white pulp were not as clear as those of the control group. However, clear boundaries were significantly restored in both NaB groups (Figure 2A). Moreover, the spleen index of the model group was significantly higher than that of the control group ($p < 0.01$; $n = 5$), whereas it was notably lower in the NaB group than in the model group (Figure 2B) ($p < 0.05$; $p < 0.05$; $n = 5$).

The expression of inflammatory cytokines is an indicator of the degree of inflammation. RT-qPCR testing and calculation of the mRNA expression of TNF-α, IL-6, IL-12, and IFN-γ revealed that the mRNA expression of cytokines in the model group was significantly higher than that in the control group ($p < 0.05$; $p < 0.001$; $p < 0.01$, $p < 0.01$; $n = 5$). Intervention with low-dose NaB ($p < 0.05$, $p < 0.01$, $p < 0.01$, $p < 0.01$; $n = 5$) and high-dose NaB ($p < 0.05$, $p < 0.001$, $p < 0.01$, $p < 0.01$; $n = 5$) resulted in significantly lower expression than that in the model group (Figure 2C–F).

NaB repairs intestinal mucosal damage

To make a more definite pathological diagnosis in mice, H&E staining was used to investigate the histopathological state of the colon in mice. H&E staining of the colon (Figure 3A) revealed serious damage in the model group compared to the control group, with observed damage including mucosal injury, crypt destruction, and cellular infiltration. Specifically, H&E staining clearly demonstrated the protective effect of NaB against colitis. After quantification, the model group had a significantly higher histopathology score than the control group ($p < 0.001$), whereas the histopathology scores in the two NaB groups were significantly lower than those in the model group ($p < 0.001$; $p < 0.001$) (Figure 3C).

The number of goblet cells in colonic crypts can reflect damage to the colonic mucosa, as reflected by AB-PAS staining [20]. From the scanning and calculation results of AB-PAS staining (Figure 3B), the number of goblet cells in the model group was much lower than that in the control group ($p < 0.001$; $n \geq 3$) (Figure 3D). Notably, the volume of goblet cells in the NaB group was significantly increased ($p < 0.01$; $p < 0.01$; $n \geq 3$).

NaB alleviates ferroptosis in colon cells of IBD mice

Ferroptosis can be assessed by measuring Fe^{2+}, GSH, SOD, MPO, and related biomarkers. The results showed that in the model group, Fe^{2+} content and MPO activity significantly increased compared to those in the control group ($p < 0.05$; $p < 0.05$; $n \geq 3$), while GSH content and SOD activity decreased ($p < 0.01$; $p < 0.001$). After NaB intervention, Fe^{2+} content ($p < 0.05$; $p < 0.05$; $n \geq 3$) and MPO activity ($p < 0.05$; $p < 0.05$; $n \geq 3$) were much lower and GSH content ($p < 0.01$; $p < 0.05$; $n \geq 3$) and SOD activity were significantly higher ($p < 0.001$; $p < 0.01$; $n \geq 3$) than those in the model group (Figure 4A–D).

Additionally, ACSL4, SLC7A11, and GPX4 are associated with ferroptosis. The model group showed significantly higher mRNA expression of ACSL4 than the control group ($p < 0.05$; $n = 5$), whereas that in both NaB groups was much lower than that in the model group ($p < 0.01$; $p < 0.01$; $n = 5$) (Figure 4E). Similarly, the mRNA expression of SLC7A11 and GPX4 was significantly lower than that in the control group ($p < 0.05$; $p < 0.05$, $n = 5$, respectively), whereas the mRNA expression of SLC7A11 ($p < 0.001$; $p < 0.001$; $n = 5$, respectively) and GPX4 ($p < 0.01$; $p < 0.01$; $n = 5$, respectively) were much higher in the NaB group than in the model group (Figure 4F,G). Similarly, the protein expression of ACSL4 in the model group was notably higher than that in the control group ($p < 0.05$; $n \geq 3$), while the protein expression of SLC7A11 ($p < 0.001$; $p < 0.001$) and GPX4 ($p < 0.01$; $p < 0.01$; $n \geq 3$) were lower in the model group than in the control group (Figure 4H–M).

NaB enhances phosphorylation of ERK and STAT3

After it was determined that IBD was alleviated by NaB, its molecular mechanism was verified by WB and

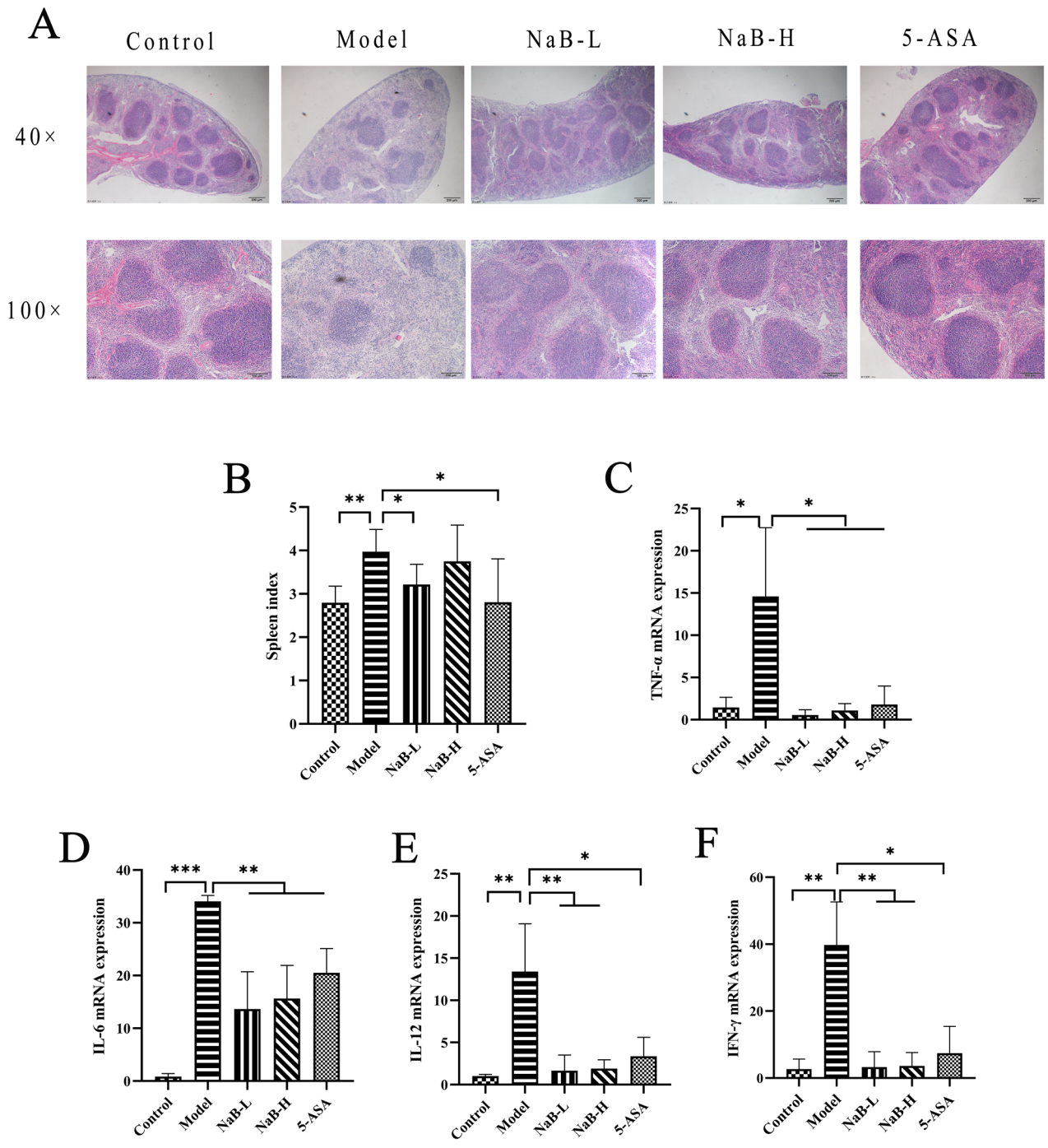

Figure 2. NaB enhanced immunity of mice and administration reduces inflammatory cytokine secretion. (A) Hematoxylin and eosin staining images of representative spleens (first line: original magnification, × 40, bar = 200 μm; second line: original magnification, × 100, bar = 100 μm). (B) Spleen index of each group. (C–F) mRNA expression level of TNF-α, IL-6, IL-12, IFN-γ. *$p < 0.05$; **$p < 0.01$; ***$p < 0.001$ vs. model.

IHC. Compared to the control group, the phosphorylation levels of ERK and STAT3 in the model group decreased significantly ($p < 0.05$; $p < 0.05$; $n \geq 3$) (Figure 5A–C). However, the phosphorylation levels of ERK ($p < 0.01$; $p < 0.05$; $n \geq 3$) and STAT3 ($p < 0.001$; $p < 0.001$; $n \geq 3$) in both the NaB groups were significantly improved quite a lot. Furthermore, IHC results for p-ERK and p-STAT3 showed that the model group exhibited weaker staining (lighter brown) than the control group. In contrast, both NaB groups displayed stronger staining (darker brown) than the model group, indicating higher expression levels of p-ERK and p-STAT3 in the control group and the two NaB groups (Figure 5D).

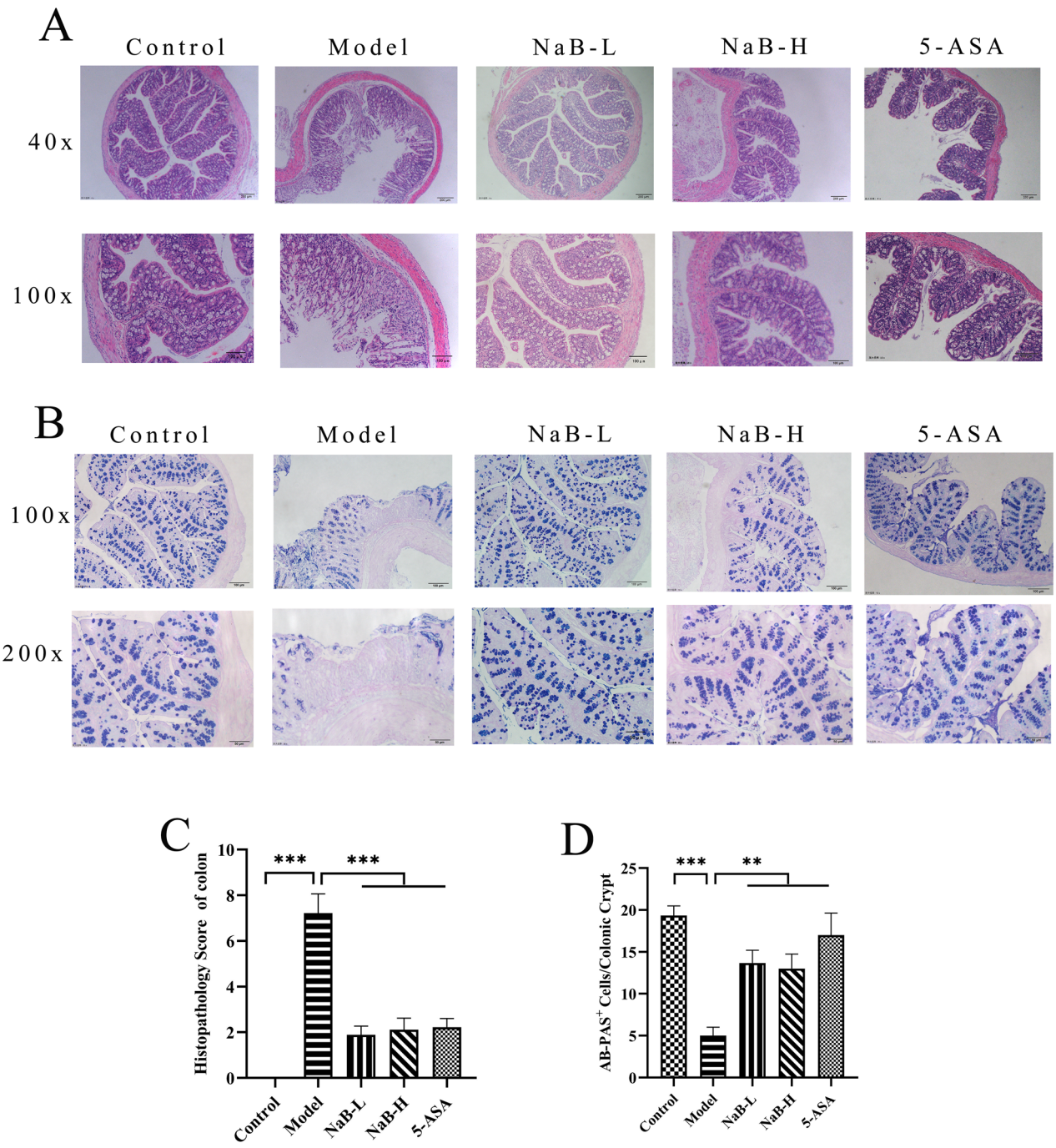

Figure 3. NaB repair intestinal mucosal damage. (A) Hematoxylin and eosin staining images of representative Colon (first line: original magnification, × 40, bar = 200 µm; second line: ORIGINAL magnification, × 100, bar = 100 µm). (B) Alcian Blue-periodic acid Schiff staining images of representative colon (first line: original magnification, × 100, bar = 100 µm; second line: original magnification, × 200, bar = 50 µm). (C) Histopathology score of colon tissue. (D) Measurement of goblet cell/crypt. *$p<0.05$; **$p<0.01$; ***$p<0.001$ vs. model.

NaB improves colonic microbiota dysbiosis in IBD

To investigate the effects of NaB on the intestinal microbiota in DSS-induced IBD mouse models, 16S rRNA sequencing was used to analyze the microbiota composition. Using the VSEARCH software, sequence clustering at 97% similarity resulted in Operational Taxonomic Units (OTUs). A Venn diagram (Figure 6A) illustrates that the total number of OUTs was 663. Specifically, the control group had a higher number of OTUs (615) than the model group (534), with 502 OTUs shared between the two groups. After the NaB intervention, the number of OTUs shared by the control group increased significantly. There were 543 OTUs in the control and NaB-L groups, and 537 OTUs in the control and NaB-H groups.

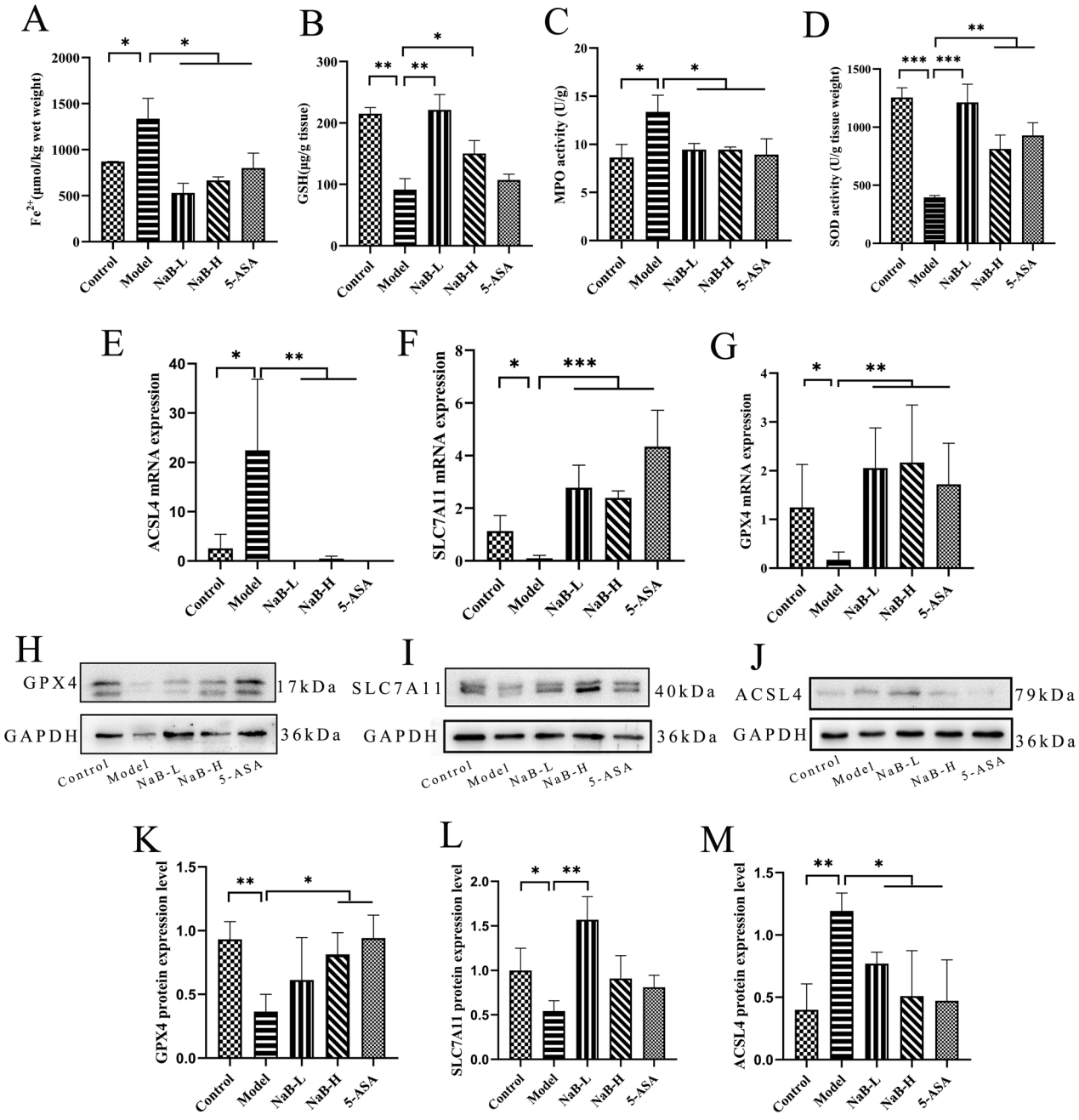

Figure 4. NaB alleviates ferroptosis in colon cells of IBD mice. (A–D) The levels of Fe^{2+}, GSH, MPO, SOD. (E–G) mRNA expression of ACSL4, SLC7A11, GPX4. (H–J) GPX4, SLC7A11, ACSL4 protein levels in colon tissues were detected by Western blotting. (K–M) Quantification of colonic relative expression of GPX4/GAPDH, SLC7A11/GAPDH, and ACSL4/GAPDH. *$p<0.05$; **$p<0.01$; ***$p<0.001$ vs. model.

The rarefaction curves, generated using indices such as the Shannon index and chao1 index, indicate the richness and diversity of the microbial populations by plotting the number of observed OTUs against the number of sequencing reads. These curves flattened, suggesting an adequate sampling depth for further analysis. In this study, the chao1 dilution curves were flattened, which indicated that the data can be further analyzed (Figure 6B). And chao1 index and ace index showed that, compared with the control group, the total population richness of the model group significantly decreased ($p<0.05$; $n=3$) (Figure 6C,D), indicating a reduction in microbial diversity following the induction of IBD.

Principal coordinate analysis (PCoA) was used to visualize the similarities and differences in the microbial community composition among the samples. Samples that clustered closely together exhibited greater similarity in their microbial communities, whereas those that were widely separated showed greater dissimilarity (Figure 6E,F). This analysis helps elucidate the extent to which NaB treatment alters gut microbiota composition in the context of IBD.

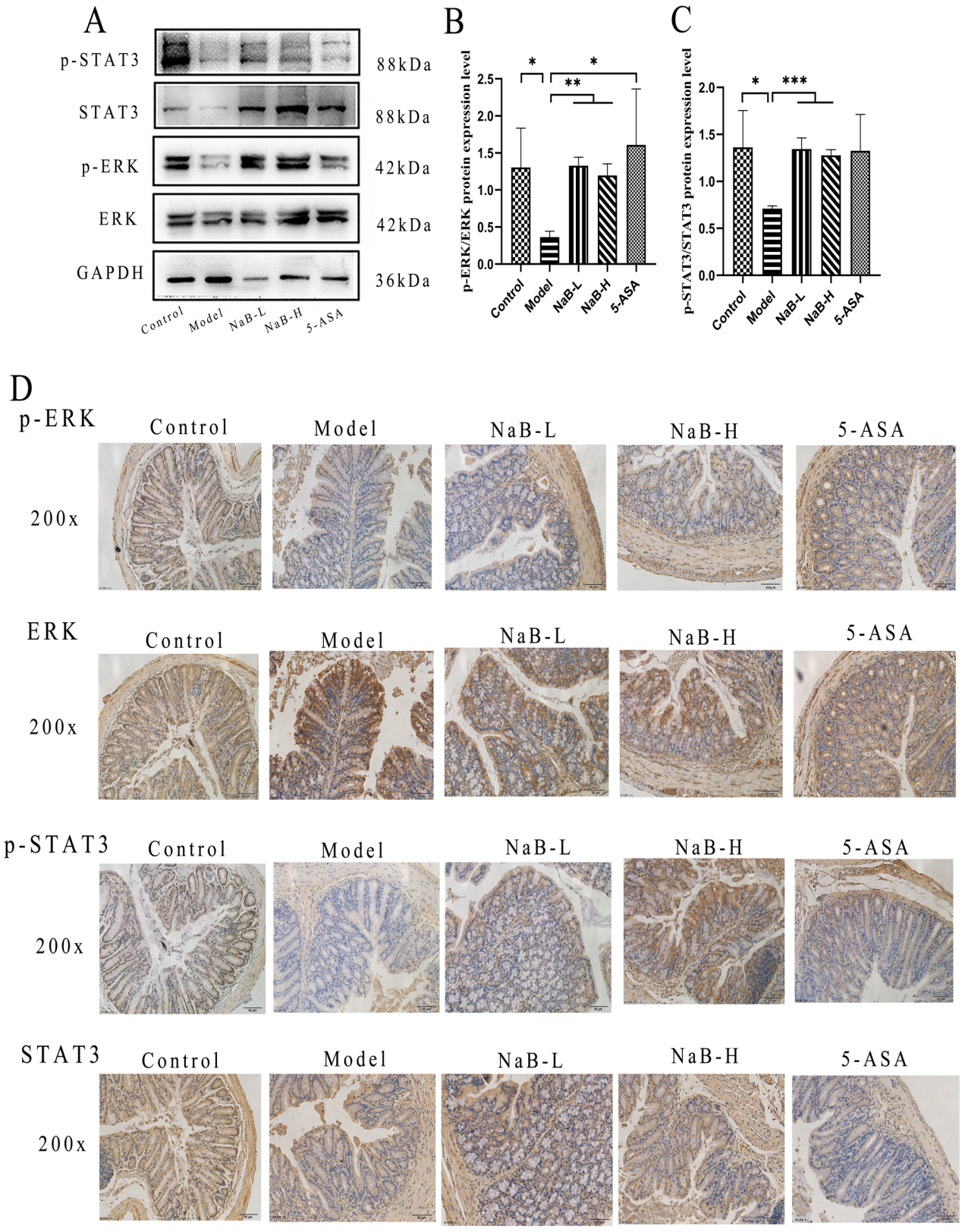

Figure 5. NaB enhance phosphorylation of ERK and STAT3. (A–C) Protein expression level of ERK, p-ERK, STAT3 and p-STAT3 detected by Western blotting. (D) Immunohistochemical results of p-ERK, ERK, p-STAT3 and STAT3 (original magnification, × 200, bar = 50 μm) *$p < 0.05$; **$p < 0.01$; ***$p < 0.001$ vs. model.

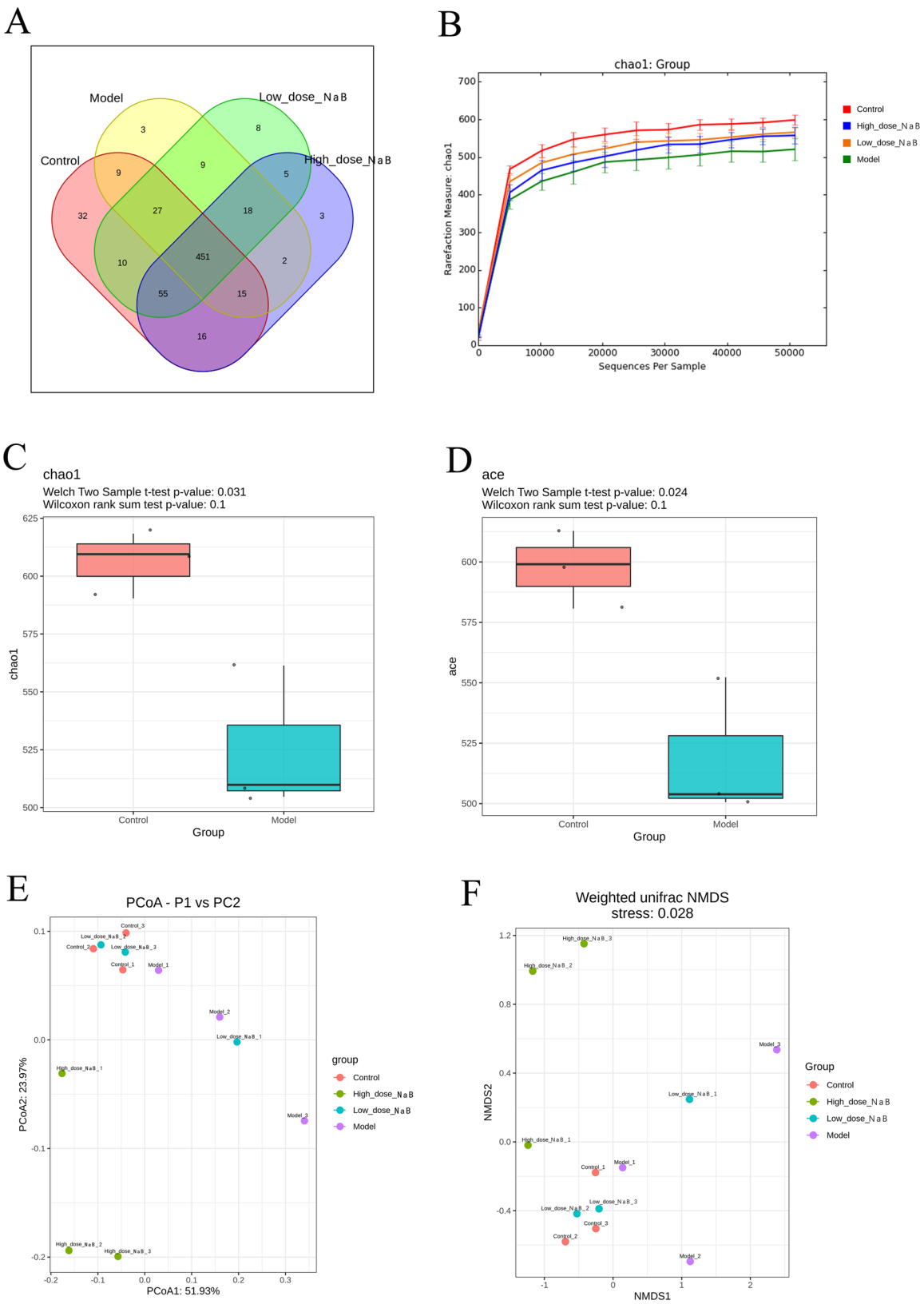

Figure 6. NaB improves colonic microbiota dysbiosis in IBD. (A) Venn diagram of OTUs of colonic microbiota. (B) Rarefaction curves plotted by chao1 index. (C–D) Comparison of chao1 index and ace index between control group and model group. (E–F) PCoA index and NMDS index of each group.

NaB improves composition of gut microbiota in IBD

Comparison of intestinal flora species and function using 16S rRNA. The histogram of LDA value distribution results indicates the species that significantly contributed to the differences between groups, specifically the biomarkers with statistical differences (Figure 7A). At the phylum level, the control group had a significantly higher abundance of *Firmicutes* than the model group ($p < 0.05$), whereas the model group showed a significantly lower abundance of *Firmicutes* than the NaB-H group ($p < 0.05$; $n = 3$) (Figure 7B). At the family level, the abundance of *Erysipelotrichaceae* in the model group was notably higher than that in the control group ($p < 0.05$; $n = 3$), whereas the NaB-H group exhibited a notably lower abundance than the model group ($p < 0.05$; $n = 3$) (Figure 7C). In addition, the model group had a significantly higher abundance of *Neisseria* and Clostridium than did the control group ($p < 0.05$; $p < 0.05$). The abundance of *Neisseria* in the NaB-L group was significantly lower than that in the model group ($p < 0.05$), and the abundance of *Clostridium* in the NaB-H group was significantly lower than that in the model group ($p < 0.05$; $n = 3$) (Figure 7D). At the species level, in contrast to the control group, the abundance of *C. cochleae* and *C. canis* in the model group was significantly increased ($p < 0.01$; $p < 0.05$; $n = 3$), the abundance of *Clostridium cocleatum* in the NaB-H group was significantly lower than that in the model group ($p < 0.01$; $n = 3$), and the abundance of *canis* bacteria in the NaB-L group was significantly lower than that in the model group ($p < 0.05$; $n = 3$) (Figure 7E–G).

In the functional analysis of the intestinal flora, in contrast to the control group, the membrane transport function of the model group was significantly weakened ($p < 0.05$; $n = 3$). The NaB-H group showed enhanced membrane transport function of IBD intestinal flora ($p < 0.05$; $n = 3$), which may be related to mucosal damage in IBD and the mucosal repair function of NaB (Figure 7H). Additionally, compared to the control group, the ATP-binding cassette (ABC) transport function was significantly weakened in the model group ($p < 0.05$; $n = 3$), while the NaB-H group showed enhanced ABC transport function in the IBD intestinal flora ($p < 0.01$; $n = 3$) (Figure 7I).

Total triterpenes possess anti-inflammatory properties, which can inhibit the inflammatory response and release inflammatory mediators, helping to reduce the symptoms and severity of inflammatory diseases. Hemiterpenes also exhibit anti-inflammatory activities. In this study, in contrast to the control group, biosynthesis of sesquiterpenes and triterpenes in the model group was notably weakened ($p < 0.01$; $n = 3$). The NaB-H group enhanced the biosynthesis of sesquiterpenoids and triterpenoids in the IBD intestinal flora ($p < 0.001$; $n = 3$), suggesting that NaB may alleviate IBD through, enhancing the synthesis of triterpenes and hemiterpenes (Figure 7J).

Discussion

Using a DSS-induced IBD mouse model, a model being used more widely in IBD studies, this study investigated the therapeutic effects of sodium butyrate (NaB) in alleviating inflammatory bowel disease (IBD) through multiple mechanisms, including ferroptosis inhibition, regulation of ERK/STAT3 signaling, and modulation of gut microbiota. Findings in our study suggest that NaB exerts beneficial effects on IBD, consistent with previous studies using different methods of administration, including intragastric delivery, which may be more effective than oral administration [21].

The spleen, a major immune organ, plays a critical role in IBD pathogenesis. In this study, NaB treatment mitigated spleen damage and reduced spleen index, indicating improved immune function. A study shows that fermented Curcuma that contains butyrate can be significantly reduce TNF-α and IgE release in DSS-Induced colitis mice, which could be related to our study [22]. Furthermore, NaB significantly reduced the secretion of pro-inflammatory cytokines, such as TNF-α, IL-1β, IL-6, and IFN-γ, which are implicated in IBD inflammation [23]. Histological analysis of the colon showed NaB restored epithelial integrity and reduced the inflammatory damage, supporting its potential as an immune-regulatory agent.

Ferroptosis, characterized by iron overload, ROS accumulation, and lipid peroxidation, has been linked to IBD pathogenesis [24,25]. Our results show that NaB reduced Fe^{2+} and MPO levels while increasing antioxidant markers like SOD and GSH, suggesting that NaB alleviates IBD by inhibiting ferroptosis. NaB also upregulated GPX4 and SLC7A11 and downregulated ACSL4, further supporting its role in ferroptosis suppression. These findings are consistent with previous studies demonstrating the beneficial effects of NaB on oxidative stress and ferroptosis in IBD [26,27]. This phenomenon is the exact opposite of NaB promoting ferroptosis in cancer and is likely related to the butyrate paradox, the contrasting effects of butyrate in different biological contexts [28].

Additionally, we explored the activation of the ERK/STAT3 signaling pathway. NaB enhanced phosphorylation

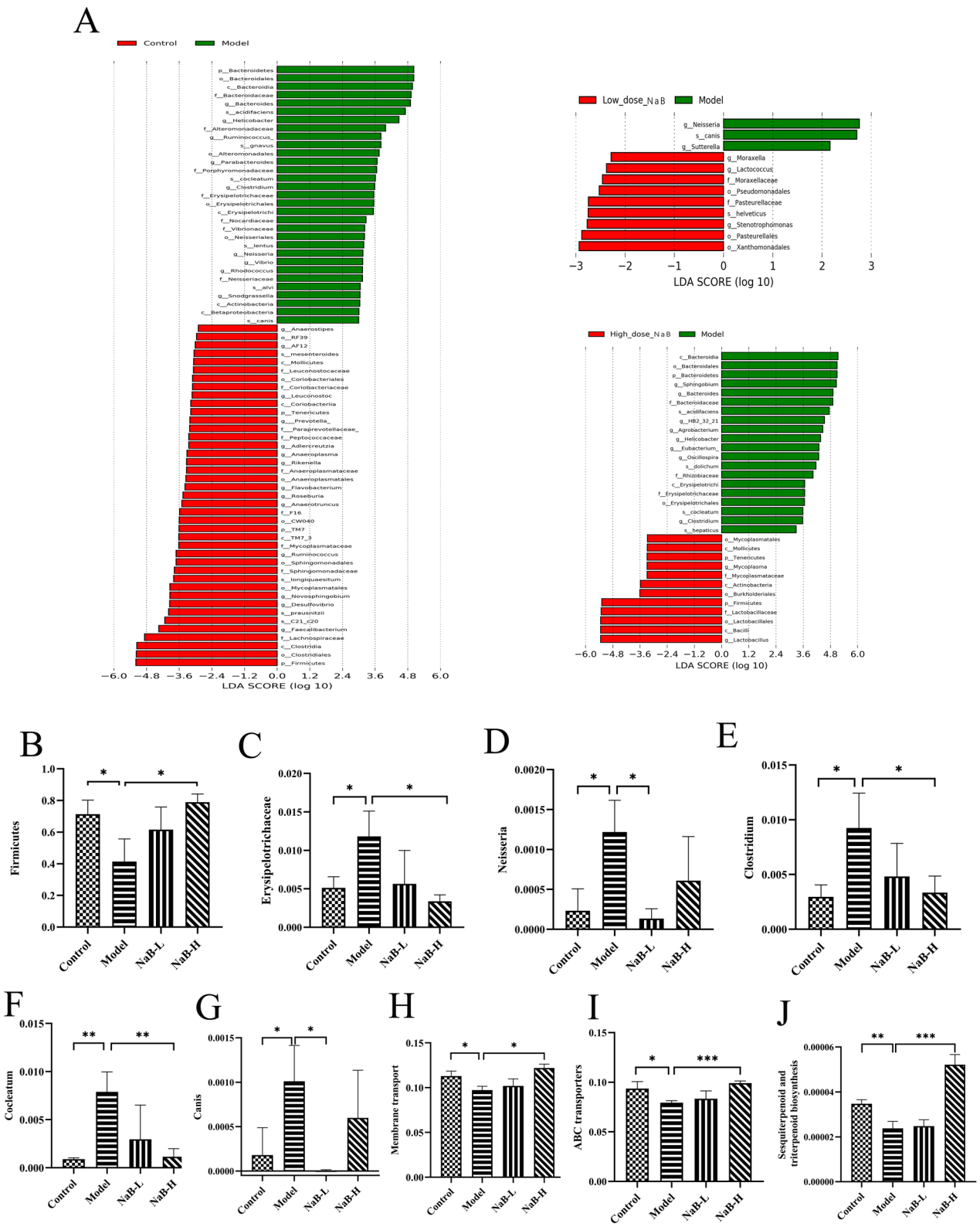

Figure 7. NaB improves composition of gut microbiota in IBD. (A) LDA score compared with model group. (B–J) Species that are representative and significantly different at phylum, family, genus and species level. *$p < 0.05$; **$p < 0.01$; ***$p < 0.001$ vs. model.

of ERK and STAT3, which are key regulators of immune function and inflammation. These findings align with studies suggesting that butyrate regulates gut barrier function through macrophage/WNT/ERK signaling [15].

As we all know, butyrate alters gene expression and arresting cell proliferation by inhibition of the chromatin-remodeling activity of histone deacetylases (HDAC). inhibition of HDAC is involved in the

anti-inflammatory effect of butyrate, which inhibits the release of proinflammatory factors. And there were studies have studied about relationship between HDAC and ERK, STAT3, however, most of them occur in cancers or other pathways [29,30]. Though there were researches have studied about pathway about ERK and STAT3 by NaB in IBD model, most of them studied about the 705 site of STAT3, which is normally triggered by JAK [31], while we mainly study about Ser727 site of STAT3. What's more, there are few studies mentioned about relationship between NaB, ERK/STAT3 and ferroptosis. According to the above analysis, in the process of alleviating IBD, NaB simultaneously inhibits ferroptosis and enhances the phosphorylation of ERK and STAT3. Combined with the database analysis of previous studies, STAT3 is the key factor of IBD and ferroptosis, and the phosphorylation of STAT3 is enhanced after the application of Fer-1, an inhibitor of ferroptosis [14]. NaB is likely to inhibit ferroptosis by enhancing ERK and STAT3 phosphorylation, and further studies are needed to elucidate the precise molecular interactions between these pathways.

The gut microbiota is a crucial modulator of IBD pathogenesis, and our results show that NaB modulated intestinal microbiota composition, notably increasing the abundance of Firmicutes, which are associated with anti-inflammatory effects, including breaking down complex carbohydrates in the diet and producing short-chain fatty acids (SCFAs) to help regulate the immune balance in the gut [32]. We also observed reductions in pro-inflammatory bacteria, such as *Clostridium cocleatum*, which is linked to intestinal mucin degradation and inflammation [33]. What's more, our results show that a low dose of NaB decreased *Erysipelotrichaceae* of in IBD mice, it may be because NaB inhibits *Erysipelotrichaceae*'s metabolites stimulating the host immune system, triggering or aggravating intestinal inflammation, and indirectly affecting intestinal barrier function and its health by affecting the composition of other flora [34] There was a study combining inulin, a kind of dietary fiber, with several intestinal bacteria in the treatment of IBD has better effects than the application of inulin alone [35], combining with the regulation of sodium butyrate on the composition and function of intestinal flora in this study, it provides us with a good idea for future therapeutic innovation. These findings suggest that NaB's impact on gut microbiota may play a significant role in its therapeutic effects in IBD.

While our results demonstrate promising effects of NaB in IBD management, further investigations are needed to confirm the molecular pathways involved, particularly the relationship between ferroptosis, ERK/STAT3 signaling, and microbiota modulation. Additionally, future studies could explore the potential for combination therapies that leverage NaB's effects on immune regulation and ferroptosis inhibition.

In conclusion, our study provides strong evidence supporting NaB as a potential adjuvant therapy for IBD, highlighting its role in regulating immune responses, preventing ferroptosis, and modulating gut microbiota. These findings open new avenues for therapeutic strategies targeting multiple pathways involved in IBD pathogenesis.

Conclusion

In summary, NaB may play a role in alleviating IBD via several mechanisms. These include inhibition of ferroptosis via increased phosphorylation of ERK and STAT3, potentially involving pathways such as macrophage/WNT/ERK signaling and mitochondrial functions, which warrant further investigation. Additionally, NaB alleviates IBD by modulating the intestinal flora, a process that could be further explored, particularly in relation to the *Clostridium cocleatum* strain.

Ethical approval

The Southern Medical University Experimental Animal Ethics Committee approved the ethical procedures and animal testing protocols for this study (SMUL202405025). This study had been conducted in accordance with the ARRIVE guidelines.

Author contributions

Yingyin Liu and Nachuan Chen conducted experiments, analyzed data, and wrote documents. Huaxing He participated in data collection and analysis. Liu and Sun conceived of and designed the study. All authors contributed to manuscript revision and approved the submitted version.

Disclosure statement

No potential conflict of interest was reported by the author(s).

Funding

This study was supported by the National Natural Science Foundation of China [No. 81773429] and Natural Science Foundation of Guangdong Province [No. 2024A1515012175]. This work was also supported by Basic and Applied Basic Research Foundation of Guangdong Province

Data availability statement

The datasets used or analyzed during the current study are available from the corresponding author upon reasonable request.

References

[1] Li Q, Wang J. The effect of protein nutritional support on inflammatory bowel disease and its potential mechanisms. Nutrients. 2024;16(14):2302. doi: 10.3390/nu16142302.

[2] Buie MJ, Quan J, Windsor JW, et al. Global hospitalization trends for Crohn's disease and ulcerative colitis in the 21st century: a systematic review with temporal analyses. Clin Gastroenterol Hepatol. 2023;21(9):2211–2221. doi: 10.1016/j.cgh.2022.06.030.

[3] Khor B, Gardet A, Xavier RJ. Genetics and pathogenesis of inflammatory bowel disease. Nature. 2011;474(7351):307–317. doi: 10.1038/nature10209.

[4] Wei H, Yu C, Zhang C, et al. Butyrate ameliorates chronic alcoholic central nervous damage by suppressing microglia-mediated neuroinflammation and modulating the microbiome-gut-brain axis. Biomed Pharmacother. 2023;160:114308. doi: 10.1016/j.biopha.2023.114308.

[5] Zhang D, Jian Y-P, Zhang Y-N, et al. Short-chain fatty acids in diseases. Cell Commun Signal. 2023;21(1):212. doi: 10.1186/s12964-023-01219-9.

[6] Vieira ELM, Leonel AJ, Sad AP, et al. Oral administration of sodium butyrate attenuates inflammation and mucosal lesion in experimental acute ulcerative colitis. J Nutr Biochem. 2012;23(5):430–436. doi: 10.1016/j.jnutbio.2011.01.007.

[7] Vagnerová K, Hudcovic T, Vodička M, et al. The effect of oral butyrate on colonic short-chain fatty acid transporters and receptors depends on microbial status. Front Pharmacol. 2024;15:1341333. doi: 10.3389/fphar.2024.1341333.

[8] Berndt C, Alborzinia H, Amen VS, et al. Ferroptosis in health and disease. Redox Biol. 2024;75:103211. doi: 10.1016/j.redox.2024.103211.

[9] Dixon SJ, Lemberg KM, Lamprecht MR, et al. Ferroptosis: an iron-dependent form of nonapoptotic cell death. Cell. 2012;149(5):1060–1072. doi: 10.1016/j.cell.2012.03.042.

[10] Long D, Mao C, Huang Y, et al. Ferroptosis in ulcerative colitis: potential mechanisms and promising therapeutic targets. Biomed Pharmacother. 2024;175:116722. doi: 10.1016/j.biopha.2024.116722.

[11] Hai S, Li X, Xie E, et al. Intestinal IL-33 promotes microbiota-derived trimethylamine N-oxide synthesis and drives metabolic dysfunction-associated steatotic liver disease progression by exerting dual regulation on HIF-1α. Hepatology. 2024; Published Ahead-of-Print. doi: 10.1097/HEP.0000000000000985.

[12] Ru Y, Luo Y, Liu D, et al. Isorhamnetin alleviates ferroptosis-mediated colitis by activating the NRF2/HO-1 pathway and chelating iron. Int Immunopharmacol. 2024;135:112318. doi: 10.1016/j.intimp.2024.112318.

[13] Hua Y, Si X, Li D, et al. Hydrogen peroxide fluorescent probe-monitored butyric acid inhibition of the ferroptosis process. Luminescence. 2024;39(3):e4715. doi: 10.1002/bio.4715.

[14] Huang F, Zhang S, Li X, et al. STAT3-mediated ferroptosis is involved in ulcerative colitis. Free Radic Biol Med. 2022;188:375–385. doi: 10.1016/j.freeradbiomed.2022.06.242.

[15] Liang L, Liu L, Zhou W, et al. Gut microbiota-derived butyrate regulates gut mucus barrier repair by activating the macrophage/WNT/ERK signaling pathway. Clin Sci. 2022;136(4):291–307. doi: 10.1042/CS20210778.

[16] Zhang G, Sheng M, Wang J, et al. Zinc improves mitochondrial respiratory function and prevents mitochondrial ROS generation at reperfusion by phosphorylating STAT3 at Ser(727). J Mol Cell Cardiol. 2018;118:169–182. doi: 10.1016/j.yjmcc.2018.03.019.

[17] Zhang WW, Thakur K, Zhang JG, et al. Riboflavin ameliorates intestinal inflammation via immune modulation and alterations of gut microbiota homeostasis in DSS-colitis C57BL/6 mice. Food Funct. 2024;15(8):4109–4121. doi: 10.1039/d4fo00835a.

[18] Li Z-Y, Lin L-H, Liang H-J, et al. Lycium barbarum polysaccharide alleviates DSS-induced chronic ulcerative colitis by restoring intestinal barrier function and modulating gut microbiota. Ann Med. 2023;55(2):2290213. doi: 10.1080/07853890.2023.2290213.

[19] Lei Y-Y, Ye Y-H, Liu Y, et al. Achyranthes bidentata polysaccharides improve cyclophosphamide-induced adverse reactions by regulating the balance of cytokines in helper T cells. Int J Biol Macromol. 2024;265(Pt 2):130736. doi: 10.1016/j.ijbiomac.2024.130736.

[20] Fang Y-X, Liu Y-Q, Hu Y-M, et al. Shaoyao decoction restores the mucus layer in mice with DSS-induced colitis by regulating Notch signaling pathway. J Ethnopharmacol. 2023;308:116258. doi: 10.1016/j.jep.2023.116258.

[21] Lee JG, Lee J, Lee A-R, et al. Impact of short-chain fatty acid supplementation on gut inflammation and microbiota composition in a murine colitis model. J Nutr Biochem. 2022;101:108926. doi: 10.1016/j.jnutbio.2021.108926.

[22] Bayazid AB, Jeong SA, Park CW, et al. The anti-inflammatory activities of fermented curcuma that contains butyrate mitigate DSS-induced colitis in mice. Molecules. 2022;27(15):4745. doi: 10.3390/molecules27154745.

[23] Agirman G, Yu KB, Hsiao EY. Signaling inflammation across the gut-brain axis. Science. 2021;374(6571):1087–1092. doi: 10.1126/science.abi6087.

[24] Zhang X, Ma Y, Lv G, et al. Ferroptosis as a therapeutic target for inflammation-related intestinal diseases. Front Pharmacol. 2023;14:1095366. doi: 10.3389/fphar.2023.1095366.

[25] Fujii J, Imai H. Oxidative metabolism as a cause of lipid peroxidation in the execution of ferroptosis. Int J Mol Sci. 2024;25(14):7544. doi: 10.3390/ijms25147544.

[26] Bian Z, Zhang Q, Qin Y, et al. Sodium butyrate inhibits oxidative stress and NF-κB/NLRP3 activation in dextran sulfate sodium salt-induced colitis in mice with involvement of the Nrf2 signaling pathway and mitophagy. Dig Dis Sci. 2023;68(7):2981–2996. doi: 10.1007/s10620-023-07845-0.

[27] Wang J, Yao Y, Yao T, et al. Hesperetin alleviated experimental colitis via regulating ferroptosis and gut microbiota. Nutrients. 2024;16(14):2343. doi: 10.3390/nu16142343.

[28] Salvi PS, Cowles RA. Butyrate and the intestinal epithelium: modulation of proliferation and inflammation in homeostasis and disease. Cells. 2021;10(7):1775. doi: 10.3390/cells10071775.

[29] Yang W, Yu T, Huang X, et al. Intestinal microbiota-derived short-chain fatty acids regulation of immune cell IL-22 production and gut immunity. Nat Commun. 2020;11(1):4457. doi: 10.1038/s41467-020-18262-6.
[30] Poria DK, Sheshadri N, Balamurugan K, ey al. . The STAT3 inhibitor static acts independently of STAT3 to decrease histone acetylation and modulate gene expression. J Biol Chem. 2021;296:100220. doi:10.1074/jbc.RA120.016645
[31] Mao H, Jia J, Sheng J, et al. Protective and anti-inflammatory role of REG1A in inflammatory bowel disease induced by JAK/STAT3 signaling axis. Int Immunopharmacol. 2021;92:107304. doi: 10.1016/j.intimp.2020.107304.
[32] Turnbaugh PJ, Ley RE, Mahowald MA, et al. Obesity-associated gut microbiome with increased capacity for energy harvest. Nature. 2006;444(7122):1027–1031. doi:10.1038/nature05414.
[33] Ma G, Hu Q, Han Y, et al. Inhibitory effects of β-type glycosidic polysaccharide from Pleurotus eryngii on dextran sodium sulfate-induced colitis in mice. Food Funct. 2021;12(9):3831–3841. doi: 10.1039/d0fo02905j.
[34] Kaakoush NO. Insights into the role of erysipelotrichaceae in the human host. Front Cell Infect Microbiol. 2015;5(84). doi:10.3389/fcimb.2015.00084
[35] Ambat A, Antony L, Maji A, et al. Enhancing recovery from gut microbiome dysbiosis and alleviating DSS-induced colitis in mice with a consortium of rare short-chain fatty acid-producing bacteria. Gut Microbes. 2024;16(1):2382324. doi: 10.1080/19490976.2024.2382324.